



HAL
open science

Infrared and Visible links for medical Body Sensor Networks

Clément Le Bas, Stéphanie Sahuguede, Anne Julien-Vergonjanne, Pierre Combeau, Lilian Aveneau

► **To cite this version:**

Clément Le Bas, Stéphanie Sahuguede, Anne Julien-Vergonjanne, Pierre Combeau, Lilian Aveneau. Infrared and Visible links for medical Body Sensor Networks. IEEE Global LIFI Congress, Feb 2018, Paris, France. hal-01704124

HAL Id: hal-01704124

<https://hal.science/hal-01704124>

Submitted on 8 Feb 2018

HAL is a multi-disciplinary open access archive for the deposit and dissemination of scientific research documents, whether they are published or not. The documents may come from teaching and research institutions in France or abroad, or from public or private research centers.

L'archive ouverte pluridisciplinaire **HAL**, est destinée au dépôt et à la diffusion de documents scientifiques de niveau recherche, publiés ou non, émanant des établissements d'enseignement et de recherche français ou étrangers, des laboratoires publics ou privés.

Infrared and Visible links for medical Body Sensor Networks

C.Lebas, S. Sahuguede, A.Julien-Vergonjanne

University of Limoges
CNRS, XLIM UMR 7252
87000 Limoges, France

P.Combeau, L.Aveneau

University of Poitiers
CNRS, XLIM UMR 7252
86000 Poitiers, France

Abstract— Our previous studies focused on channel simulation and performance evaluation of optical wireless links for medical body sensor networks. This allowed us to increase our expertise in this field and to propose here a full optical wireless bidirectional system named as LiFi communication system for medical monitoring applications. The full duplex bidirectional communication is based on an infrared uplink and visible downlink. The studied scenario considers a patient wearing both an infrared transmitter connected to a medical sensor and a visible light receiver. The infrared receivers and visible light emitters are included in light fixtures at the ceiling. The study relies on channel modelling considering patient body features, locations and movements. Using ray-tracing technique associated to Monte-Carlo method, we determine the overall performance in terms of outage probability. We apply our methodology considering various medical sensors and show that it is possible to satisfy the overall quality of service in terms of bit error rate and data rate.

Keywords—LiFi for medical applications; infrared transmissions; channel modelling;

I. INTRODUCTION

Optical Wireless Communication (OWC) in the nanometer-range from ultra-violet to InfraRed (IR) has the potential to become a complement or alternative to RF technology [1]. Recently, OWC has gained popularity in the visible range domain named Visible Light Communication (VLC), due to the dual use of Light Emitting Diode (LED) devices for both illumination and wireless communications. This technology, named as LiFi communication offers many benefits such as unlicensed spectrum, high bandwidth, simple and cheap front-ends and no electromagnetic interference. This latter benefit is important when considering portable medical monitoring devices incorporating wireless transmission technologies. Indeed, the use of RF technologies around the human body can be problematic in terms of impact on health, security and confidentiality. Therefore, OWC technology can be a solution to provide low cost, efficient and safe communications for medical devices, between medical equipment or between patients and monitoring stations [2-10].

Involved in OWC field for medium and low-rate medical applications, we have developed skills and dedicated tools to address the modelling of indoor optical wireless channels applied to Body Sensor Networks (BSN) [6]. By using robust mathematical models (Monte-Carlo, Metropolis, etc.), our team has developed RaPSor (Ray Propagation Simulator) software

which is an open and extensible tool, based on the Netbeans platform for the modelling of Infrared and Visible links [11]. We have also designed portable OWC devices to carry out experimental test-beds for low data rates infrared uplinks exploiting indoor diffuse reflections [12].

In this study, we propose a full optical BSN based on bidirectional LiFi communication system using IR technology and VLC for indoor health monitoring. A diffuse IR transmitter ensures the uplink between a wearable medical sensor and receivers included in VLC-ready light fixtures. Visible downlinks from the luminaires allow sending medical data to a VLC receiver also carried by the monitored patient. In the study, we focus on parameters affecting IR and VLC channel behavior related to the presence of patient body wearing the IR/VLC transceivers and to the locations and movements inducing orientation variations of the IR emitter and VLC receiver. System consumption and thus emitted power is also of main concern in order to meet power standards and extend usage time.

We investigate these issues by simulation using RaPSor and discuss the overall IR / VLC performance considering various medical monitoring constraints and lighting conditions. In particular, we determine whether it is possible to establish VLC transmissions with very low power levels so that the light is quite not perceptible by the human eye.

The paper is organized as follows. The system description we investigate is presented in section 2. Section 3 focuses on the theoretical analysis of IR uplink and VLC downlink channels considering patient body presence and movements. Section 4 reports the study of overall performance before conclusion in section 5.

II. SYSTEM DESCRIPTION

To evaluate the overall performance of IR/VLC for health monitoring, we consider the scenario illustrated in Fig. 1.

The studied area has dimensions of $(5 \times 5 \times 3)$ m³ (length, width, height) which is a typical one. Four LED based luminaires are located at the ceiling (coordinates are indicated in TABLE I) oriented towards the floor. The LED radiation patterns are modeled by a Lambertian one with an order $m=1$ that corresponds to a half-power angle of 60°.

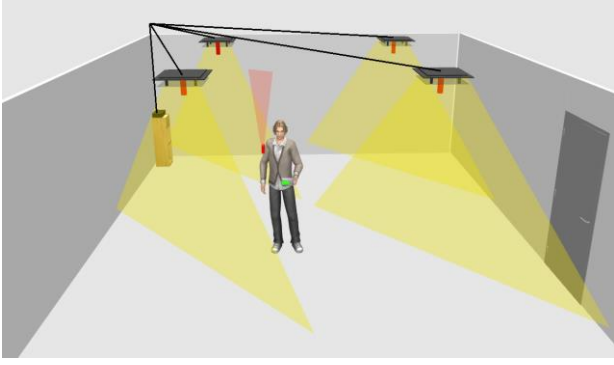


Fig. 1. Environment description for the bidirectional full optical link

In the studied scenario, the visible downlinks are established between LEDs and a VLC receiver integrated into a tablet for example worn by a patient moving in the environment. To represent this scenario we will model the patient body considering random positions in the environment. In addition, the receiver is located at a distance of 20cm from the body and 1.2m from the floor. As the patient is moving, it is possible that the orientation of the receiver varies. Receiver orientation can be defined through polar and azimuthal angles. Consequently, we will consider random values of these two angles taken in the ranges defined in TABLE I, which also lists the values taken for responsivity R , Field-Of-View (FOV) and physical area of the photodetector which are typical values for VLC receivers. For simplicity and without loss of generality we will not model furniture.

TABLE I. VLC system parameters

VLC Transmitters	Coordinates [x y z] (m)	T1 : [1.25 1.25 3] T2 : [1.25 3.75 3] T3 : [3.75 3.75 3] T4 : [3.75 1.25 3]
	Half-power angle $\varphi_{1/2}$	60°
VLC Receiver	Responsivity R	0.48 A/W
	Field of View (FOV)	65°
	Physical surface area	1cm ²
	Range of polar angle θ	$[0, \pi/3]$
	Range of azimuthal angle φ	$[0, 2\pi]$
	Height of receiver from the floor	1.2m

Concerning IR uplink transmission, we suppose an emitter integrated into a medical device worn by the patient at the shoulder (1.5m from the floor), and four IR receivers located at the same coordinates as the luminaires (see TABLE II which also reports the typical parameters taken for IR receivers such as responsivity R , FOV, physical area). In addition, we use one of the simplest combining techniques which is Switching

Combining (SwC) selecting only once the information if one or several receivers correctly receive it.

Besides, because patient movements, the wearable emitter orientation can vary, which is taken into account through polar and azimuthal angles (see TABLE II). Note that as the sensor is worn at the shoulder, the variation range of azimuthal angle is restricted compare to VLC receiver case. Furthermore, it is supposed that the IR emitter pattern is Lambertian with an optimal m order equal to 2 that is an half-power angle of 45° [14].

Among the specifications of medical remote monitoring applications, it can be noted that the bit rates are generally less than 10 Mbps but with a rather high quality of service [6]. For this low data rates and considering typical impulse responses length and mean delay spreading, we can neglect inter-symbol interference in both IR and VLC cases. The channels are characterized by the optical DC gain, defined as :

$$H(0) = \int_{-\infty}^{+\infty} h(t) dt = H_0 \quad (1)$$

where $h(t)$ represents the channel impulse response.

Patient mobility induces different link configurations related to patient positions and orientations of VLC receiver and IR emitter. Consequently, the optical DC gain is a random variable. In the following, we study the channel statistical behavior taking also into account the human body model.

TABLE II. IR system parameters

IR Transmitter	Half-power angle $\varphi_{1/2}$	45°
	Height of Emitter from the floor	1.5m
	Range of polar angle θ	$[0, \pi/3]$
	Range of azimuthal angle φ	$[0, \pi]$
IR Receivers	Coordinates [x y z] (m)	R1 : [1.25 1.25 3] R2 : [1.25 3.75 3] R3 : [3.75 3.75 3] R4 : [3.75 1.25 3]
	Responsivity R	1 A/W
	Field of View (FOV)	45°
	Physical surface area	34.5mm ²

III. IR UPLINK AND VLC DOWNLINK CHANNELS

A. Overall concepts

In order to study the IR and VLC channels, we used a ray-tracing based simulator developed in XLIM laboratory. It allows determining the impulse response $h(t)$ for a defined

scenario by using stochastic method of Monte Carlo, associated to ray tracing algorithm [11,14].

For all the simulations, in order to manage tradeoffs between calculation times and accuracy, we consider three reflections per optical beam, which is a classical approach for non-directed Line-Of-Sight (LOS), or diffuse transmissions. Furthermore, the wall material is plaster surface with reflectivity fixed to 0.73 and the floor material is plastic one with a reflectivity set to 0.18 [15].

Due to patient mobility inside the room, we will consider a set of impulse responses $h(t)$ of IR and VLC links obtained with ray-tracing simulations. A number of 1000 random positions has been taken since it has been verified that it permits to have convergent results. The angle variation step for the orientation changes of the IR transmitter and the VLC receiver is set to $\pi/6$. The channel behavior will be then characterized by means of H_0 statistical distribution in terms of probability density function (PDF) and cumulative density function (CDF).

Our objective is to analyze the link reliability from CDF. It will be higher the more the $CDF(H_0)$ will be small for a given H_0 since the goal is to reach high DC gain H_0 values with a high probability.

B. IR channel

To study the impact of the human body on the IR channel, we have to model its geometry and its reflectance properties. It is important to take into account the width of the body because of possible blocking effects since receiver is supposed to be at the shoulder; however, level of details is not important for evaluating channel gain when considering low data rates [16, 22]. We thus consider the body shape as illustrated in Fig.2 but with a given width of 20 cm. For the reflectivity, since there is a large range of possible values depending on the skin and the clothes, we have taken two extreme values i.e. $\rho_{b1}=0.1$ and $\rho_{b2}=0.9$.

These two cases are compared in the following to the reference case where neither the body nor the variations of emitter orientation are taken into account, as summarized in Fig.2.

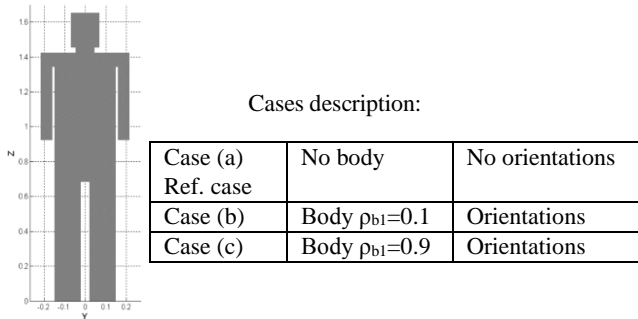


Fig. 2. Shape of the body for IR and VLC modeling and cases description

To determine the DC gain we define H_i as being the DC gain between given position and orientation of the IR emitter and the receiver R_i with i varying from 1 to 4. In order to take into

account the SwC method, we define H_{0-IR} which corresponds to the best DC gain considering the four active receivers:

$$H_{0-IR} = \text{Max}[H_1, H_2, H_3, H_4] \quad (2)$$

As the emitter position is random, H_{0-IR} follows a statistical distribution $p(H_{0-IR})$. The CDF of the gain H_{0-IR} can be thus expressed as:

$$CDF(H_{0-IR}) = \int_{-\infty}^{H_0} p(H_{0-IR}) dH_{0-IR} \quad (3)$$

We have reported in Fig.3 the evolution of $PDF(H_{0-IR})$ and $CDF(H_{0-IR})$ for all the studied cases defined in Fig.2.

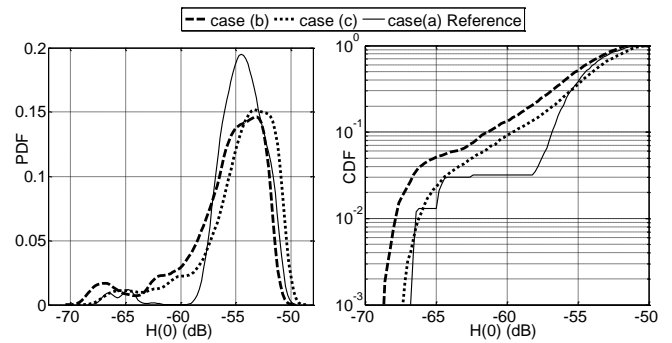


Fig. 3. H_{0-IR} Probability Density Function and Cumulative Density Function

It can be seen that the presence of the body and variations in the orientation of the transmitter affect the statistical distribution and the values of DC gain. This impact is all the more negative as the reflectivity of the body is weak.

C. VLC channel

For the VLC channel, we consider the same body shape as presented for IR but we do not model the width of the body. Actually, the VLC receiver is here supposed to be in front of the body and not over the body as previously for IR emitter.

We compare the same cases as for the IR channel described in Fig.2 but here orientation variations are related to VLC receiver instead of IR emitter.

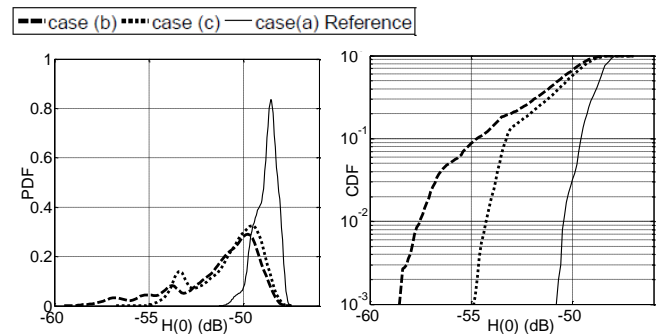


Fig. 4. H_{0-VLC} Probability Density Function and Cumulative Density Function

We can see in Fig.4 compared to Fig. 3 that the impact of the body and the orientation changes is much more significant for the VLC downlink than for the IR uplink. Another difference is that the effect is important even if the reflectivity of the body is high.

To compare VLC and IR link behaviors, we have plotted in Fig.5 the two PDF corresponding to case (b) – with orientation changes and body reflectivity $\rho_{b1}=0.1$ - for both channels gains H_{0-VLC} and H_{0-IR} . We observe that VLC downlink globally overcomes IR uplink since channel gain values are higher most of the time. However, performance also depends on the emitted power of both links and the receiver characteristics. In the next part, we will investigate the global performance of the dual link IR/VLC to discuss the possibility of establishing downlinks with a VLC emission power that is sufficiently low to consider that the lighting is not very noticeable. This is important because the application must be able to operate whatever the lighting level in the room. For the IR uplink system, the challenge is also to reduce as much as possible the emitted power to decrease the consumption of the device carried by the patient.

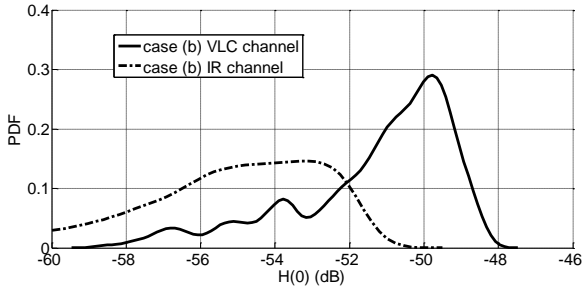


Fig. 5. H_{0-VLC} and H_{0-IR} Probability Density Function for case (b)

IV. SYSTEM PERFORMANCE ANALYSIS

A. Outage probability definitions

As DC gain randomly varies because of mobility, the Signal to Noise Ratio (SNR) also follows a statistical distribution. Thus, we focus on outage probability which is a common metric to evaluate the link performance. It is defined by [17]:

$$P_{out} = p(SNR < SNR_0) \quad (4)$$

Where SNR_0 represents the threshold SNR needed to support a given bit data rate R_b . Thus, P_{out} can be seen as a function of SNR_0 and is impacted by average emitted power P_t , data rate and ambient noise characterized by its power spectral density N_0 .

Considering On-Off Keying (OOK) modulation, SNR can be expressed as:

$$SNR = \frac{P_t^2 H_0^2 R^2}{4N_0 R_b} \quad (5)$$

The photodiode at the reception converts the optical signal to

an electrical signal adding thermal and shot noise. Generally, shot noise is the most preponderant due to the ambient photo-current I_B whose value depends on wavelength. A conventional value of N_0 is given by:

$$N_0 \approx 2qI_B \quad (6)$$

Where q is the electron quantum charge. We will consider in this study typical values of I_B around $5100\mu A$ for VLC and $200\mu A$ for near-infrared wavelengths [18].

From the distribution of H_0 for each channel established previously, we will consider the distributions $p(SNR_{IR})$ $p(SNR_{VLC})$ obtained using (5) and so we can define two outage probabilities P_{out-IR} and $P_{out-VLC}$ corresponding to the link performance of IR and VLC channels:

$$P_{out-IR} = p(SNR_{IR} < SNR_{0-IR}) \quad (7)$$

$$P_{out-VLC} = p(SNR_{VLC} < SNR_{0-VLC}) \quad (8)$$

Where SNR_{0-IR} , respectively SNR_{0-VLC} , is the SNR needed on the IR link, respectively VLC link, to support a given bit rate R_{b-IR} in the uplink, respectively R_{b-VLC} in the downlink.

In order to analyze the performance of the whole bidirectional communication system, we define global outage probability traducing that there is a failure either on one link or on the other. The global outage probability P_{out} is thus the probability that the SNR drops below the threshold value on any of the link. We can express it as:

$$\begin{aligned} P_{out} &= p\left(\begin{array}{l} SNR_{IR} < SNR_{0-IR} \cup SNR_{VLC} \\ < SNR_{0-VLC} \end{array}\right) \\ &= p\left(\begin{array}{l} SNR_{IR} < SNR_{0-IR} \\ < SNR_{0-VLC} \end{array}\right) + p\left(\begin{array}{l} SNR_{VLC} \\ < SNR_{0-VLC} \end{array}\right) \\ &\quad - p\left(\begin{array}{l} SNR_{IR} < SNR_{0-IR} \\ < SNR_{0-VLC} \end{array}\right) \cdot p\left(\begin{array}{l} SNR_{VLC} \\ < SNR_{0-VLC} \end{array}\right) \\ &= P_{out-IR} + P_{out-VLC} - P_{out-IR} \cdot P_{out-VLC} \end{aligned} \quad (9)$$

Here, P_{out} is a function of a couple $(SNR_{0-IR}, SNR_{0-VLC})$. For each link, they depend on average emitted power (P_{t-IR} , and P_{t-VLC}), data rate (R_{b-IR} and R_{b-VLC}) and ambient noise power.

Here, P_{out} is a function of a couple $(SNR_{0-IR}, SNR_{0-VLC})$. For each link, they depend on average emitted power (P_{t-IR} , and P_{t-VLC}), data rate (R_{b-IR} and R_{b-VLC}) and ambient noise power.

In the following analysis, we will consider that for the studied medical BSN, we have the same required data rate on both links: $R_{b-IR} = R_{b-VLC} = R_b$.

In addition, we assume that the targeted BER are the same for the two channels. So, considering the same OOK modulation for both links this means that $SNR_{0-IR} = SNR_{0-VLC}$.

B. Global performance analysis

Our objective is to study the possibility of establishing bidirectional full optical IR/VLC link with VLC downlink emission power sufficiently low to consider that the light is not turned on or is not very noticeable. This is important because the application must be able to operate whatever the lighting level in the room including night conditions. For the IR uplink system, the challenge is also to reduce as much as possible the emitted power to decrease the consumption of the worn device in order to have the greatest possible lifetime.

As an example, we focus on the minimal powers for IR and VLC links (P_{t-IR} and P_{t-VLC}) needed to achieve a given global outage probability value using (9), for $R_b = 1$ Mbps and $SNR_{0-IR} = SNR_{0-VLC} = 16.1$ dB ($BER \approx 10^{-10}$ for OOK). This corresponds to classical BSN requirements for medical applications that should support bit rates in the range of 10 kbps to 1Mbps with very low BER [19]. To illustrate more precisely VLC power corresponding to real use cases, instead of using P_{t-VLC} we have illustrated results in terms of corresponding average lighting level E_{mean} in lux, within the room at the height of 1.2m [20].

All the couples of the minimal values (E_{mean} ; P_{t-IR}) are plotted in Fig.6 for respectively $P_{out} = 0.1\%$, 1% and 10% when for both links the body reflectivity is set to $\rho_{b2}=0.9$.

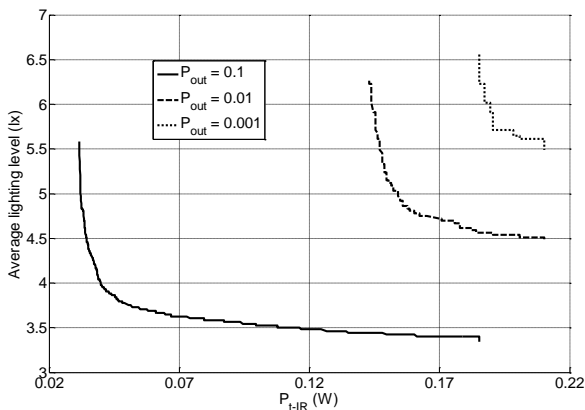


Fig. 6. Evolution of the minimal needed P_{t-IR} as a function of the associated minimal illumination E_{moy} in order to respect $BER=10^{-10}$. $\rho_{b2}=0.9$

Obviously, it can be seen that to guarantee a certain overall quality of service for the IR / VLC transmission, if the IR power is decreased, the lighting level of the room must be increased.

Concerning the value of P_{t-IR} that can be chosen, we can remark that it is always below the eye safety constraints of around 300mW for IR source with half-power angle of 45° . Moreover, the minimum possible value of P_{t-IR} is as much lower as the target P_{out} is high. We can also remark that for this lowest IR power value, the corresponding VLC power must highly be increased, illustrating the tradeoff between both power constraints. On the other side, the minimal value of E_{mean} as the range of lighting values also depend on the P_{out} .

Same results have been obtained for the other value of reflectivity coefficient $\rho_{b2}=0.1$ and the conclusions are quite the same for P_{t-IR} . However, E_{mean} required values are significantly increased to satisfy the targeted P_{out} .

The lowest limit values of P_{t-IR} , respectively E_{mean} , corresponding to a maximal average lighting, respectively a maximal IR power, are reported in TABLE III for different medical application types and for the two extreme values of ρ_b .

These results highlight that, for data rates lower than 1Mbps, specifications with low IR emitted power can be satisfied, which is of great importance for consumption. In addition, we show that low VLC powers for downlink are sufficient so that the illumination is almost imperceptible by human eye. For some cases (in bold) it may not be possible to respect IR and/or VLC constraints respectively for eye safety and night watch use [21]. These limitations will mostly depend on body's reflectivity value and the targeted P_{out} .

Table III. Examples of performance for medical sensor applications

P_{out}	$\rho_{b2}=0.1$		$\rho_{b2}=0.9$	
	E_{mean} (Lx)	P_{t-IR} (mW)	E_{mean} (Lx)	P_{t-IR} (mW)
Accelerometer, blood pressure, SPO2, temperature $R_b < 10\text{kbps}$; $BER < 10^{-10}$				
10^{-1}	0.48	4	0.3	2.6
10^{-2}	1.4	20	0.45	13.5
10^{-3}	2.4	25.3	0.55	18
Electrocardiogram (ECG); $R_b=72$ kbps; $BER < 10^{-10}$				
10^{-1}	1.3	12.6	0.9	7.6
10^{-2}	3.7	56	1.2	38.3
10^{-3}	6.5	67.8	1.4	50
Electromyogram (EMG); $R_b=1.5$ Mbps; $BER < 10^{-10}$				
10^{-1}	5.9	48	4.1	32
10^{-2}	16.8	236	5.5	145
10^{-3}	29.6	301	6.7	220
Video; $R_b=10$ Mbps; $BER < 10^{-3}$				
10^{-1}	7.8	55	5.4	38
10^{-2}	22.2	331	7.2	223
10^{-3}	39.2	430	8.9	293

V. CONCLUSION

The results presented in this article illustrate the impact of two very important parameters for the performance of a communicating mobile full-optical wireless system with transmitters and receivers worn by a person. It is the presence of the body and its optical reflectivity properties as well as variations of direction of the transceivers induced by the movements. This study was conducted for a bidirectional system involving an IR uplink and a VLC downlink in indoor environment. Furthermore, we consider health monitoring applications.

First, we have analyzed the statistical behavior of both IR and VLC channel thanks to ray-tracing simulations, allowing modeling LOS and Non-LOS links. The results showed that it is important for the IR or the visible channels, to model the presence of the body and the changes of orientations related to the movements of the body. On the other hand, the impact of the reflectivity of the body is much more significant on the VLC downlink than on the IR uplink for which the transmitter is on the shoulder.

Then, the channel statistics were used to determine the overall performance in terms of outage probability jointly considering IR uplink and visible downlink transmissions.

In particular, we focused on a scenario where the data rates and the required quality of service for both links were identical. The analysis of this overall performance was done by examining the power-related issues for infrared and visible and seeking to minimize both emitted optical powers.

We have pointed out that for bit rates lower than 1 Mbps, it is possible to follow the medical data of a mobile patient with low power emitted in IR, which is very important for reasons of consumption since the system is worn. In addition, we have shown that low VLC downlink powers are possible, which means that in this case the illumination is very little perceptible to the human eye. Some use cases such as the video application, however, require a high transmitted IR power, which does not satisfy the eye safety, or a too high level of illumination if the targeted performance is high. However, our study concludes that for most medical sensors, the proposed system is able to satisfy the overall quality in terms of bit error rate and data rate, which makes the proposed Li-Fi communication system promising.

REFERENCES

- [1] M. Uysal, C. Capsoni, Z. Ghassemlooy, A.C. Boucouvalas, E. G. Udvary (Eds.), *Optical Wireless Communications – An Emerging Technology*, Springer, 2016.
- [2] R. Murai *et al.*, "A novel visible light communication system for enhanced control of autonomous delivery robots in a hospital," *2012 IEEE/SICE International Symposium on System Integration (SII)*, Fukuoka, 2012, pp. 510-516.
- [3] Y. K. Cheong, X. W. Ng and W. Y. Chung, "Hazardless Biomedical Sensing Data Transmission Using VLC," in *IEEE Sensors Journal*, vol. 13, no. 9, pp. 3347-3348, Sept. 2013.
- [4] J. Song *et al.*, "Indoor hospital communication systems: An integrated solution based on power line and visible light communication," *2014 IEEE Faible Tension Faible Consommation*, Monaco, 2014, pp.1-6.
- [5] YY.Tan, WY Chung, "Mobile health-monitoring system through visible light communication." *Bio-medical materials and engineering* 24(6):3529-38 · September 2014
- [6] L. Chevalier, S. Sahuguede and A. Julien-Vergonjanne, "Optical Wireless Links as an Alternative to Radio-Frequency for Medical Body Area Networks," in *Selected Areas in Communications, IEEE Journal on*, vol.33, no.9, pp.2002-2010, Sept. 2015, doi: 10.1109/JSAC.2015.2432527
- [7] W. A. Cahyadi, T. I. Jeong, Y. H. Kim, Y. H. Chung and T. Adiono, "Patient monitoring using Visible Light uplink data transmission," *2015 International Symposium on Intelligent Signal Processing and Communication Systems (ISPACS)*, Nusa Dua, 2015, pp. 431-434.
- [8] A. Al-Qahtani *et al.*, "A non-invasive remote health monitoring system using visible light communication," *2015 2nd International Symposium on Future Information and Communication Technologies for Ubiquitous HealthCare (Ubi-HealthTech)*, Beijing, 2015, pp.1-3
- [9] D. R. Dhatchayeny, A. Sewaiwar, S. V. Tiwari and Y. H. Chung, "EEG biomedical signal transmission using visible light communication," *2015 International Conference on Industrial Instrumentation and Control (ICIC)*, Pune, 2015, pp. 243-246.
- [10] T. Adiono, R. F. Armansyah, S. S. Nolika, F. D. Ikram, R. V. W. Putra and A. H. Salman, "Visible light communication system for wearable patient monitoring device," *2016 IEEE Region 10 Conference (TENCON)*, Singapore, 2016, pp. 1969-1972.
- [11] A. Behloul, P. Combeau and L. Aveneau, "MCMC Methods for Realistic Indoor Wireless Optical Channels Simulation," in *Journal of Lightwave Technology*, vol. 35, no. 9, pp. 1575-1587, May1, 1 2017.doi: 10.1109/JLT.2017.2662939
- [12] C. Le Bas, S. Sahuguede and A. Julien-Vergonjanne "Theoretical and Experimental Approach for the Design of an Optical Wireless Physical Activity Monitoring System", *International Journal of Wireless Information Networks* 2017, doi: 10.1007/s10776-017-0337-4
- [13] D. Wu, et al., "Effect of optimal Lambertian order for cellular indoor optical wireless communication and positioning systems", *Opt. Eng.* 55 (6), 066114 (2016)
- [14] A. Behloul, P. Combeau, L. Aveneau, S. Sahuguede and A. Julien-Vergonjanne, "Efficient simulation of optical wireless channel, Application to WBANs with MISO link", *Procedia Computer Science*, vol. 40, pp 190-197 (2014)
- [15] K. Lee, H. Park and J. R. Barry, "Indoor Channel Characteristics for Visible Light Communications," in *IEEE Communications Letters*, vol. 15, no. 2, pp. 217-219, February 2011. doi: 10.1109/LCOMM.2011.010411.101945
- [16] C. Le Bas, S. Sahuguede, A. Julien-Vergonjanne, A. Behloul, P. Combeau and L. Aveneau, "Human body impact on mobile visible light communication link," *2016 10th International Symposium on Communication Systems, Networks and Digital Signal Processing (CSNDSP)*, Prague, 2016, pp. 1-6.doi: 10.1109/CSNDSP.2016.7573900
- [17] A. Goldsmith, *Wireless Communications*. Cambridge University Press, 2005
- [18] A. J. C. Moreira, R. T. Valadas and A. M. de Oliveira Duarte, "Characterisation and modelling of artificial light interference in optical wireless communication systems," *Proceedings of 6th International Symposium on Personal, Indoor and Mobile Radio Communications*, Toronto, Ont., 1995, pp. 326-331 vol.1. doi: 10.1109/PIMRC.1995.476907
- [19] A.Julien-Vergonjanne, S.Sahuguede, L.Chevalier "Optical Wireless Body Area Networks for Healthcare Applications" in *Optical Wireless Communications : An emerging technology* Springer International Publishing, chap.26, pp 569-587, Aug.2016
- [20] B. Hussain, X. Li, F. Che, C. Patrick Yue and L. Wu, "Visible Light Communication System Design and Link Budget Analysis," in *Journal of Lightwave Technology*, vol. 33, no. 24, pp. 5201-5209, Dec.15, 15 2015
- [21] http://www.ageta.lt/app/webroot/files/uploads/filemanager/File/info/EN_12464-1.pdf
- [22] A. Behloul, P. Combeau, S. Sahuguede, A. Julien-Vergonjanne, C. Le bas and L. Aveneau, "Impact of Physical and Geometrical Parameters on Visible Light Communication Links", *Proceedings of IEEE RTUWO conference*, pp 73-79, 2-3 november 2017, Riga, Latvia.